THE JOURNAL OF BIOLOGICAL CHEMISTRY
Vol. 275, No. 28, Issue of July 14, pp. 21355–21363, 2000

*Printed in U.S.A.*

# Agonist-induced Isomerization in a Glutamate Receptor Ligand-binding Domain

## A KINETIC AND MUTAGENETIC ANALYSIS*

Received for publication, December 10, 1999, and in revised form, March 20, 2000
Published, JBC Papers in Press, March 28, 2000, DOI 10.1074/jbc.M909883199

**Rupert Abele‡§, Kari Keinänen¶, and Dean R. Madden‡‖**

*From the ‡Ion Channel Structure Research Group, Max Planck Institute for Medical Research, Jahnstrasse 29, 69120 Heidelberg, Germany and the ¶Viikki Biocenter, Department of Biosciences, Division of Biochemistry, and the Institute of Biotechnology, University of Helsinki, FIN-00014 Helsinki, Finland*

**Agonist binding to glutamate receptor ion channels occurs within an extracellular domain (S1S2) that retains ligand affinity when expressed separately. S1S2 is homologous to periplasmic binding proteins, and it has been proposed that a Venus flytrap-style cleft closure triggers opening of glutamate receptor ion channels. Here we compare the kinetics of S1S2-agonist binding to those of the periplasmic binding proteins and show that the reaction involves an initial rapid association, followed by slower conformational changes that stabilize the complex: "docking" followed by "locking." The motion detected here reflects the mechanism by which the energy of glutamate binding is converted into protein conformational changes within S1S2 alone. In the intact channel, these load-free conformational changes are harnessed and possibly modified as the agonist binding reaction is used to drive channel opening and subsequent desensitization. Using mutagenesis, key residues in each step were identified, and their roles were interpreted in light of a published S1S2 crystal structure. In contrast to the Venus flytrap proposal, which focuses on motion between the two lobes as the readout for agonist binding, we argue that smaller, localized conformational rearrangements allow agonists to bridge the cleft, consistent with published hydrodynamic measurements.**

Glutamate receptor ion channels (GluR)[1] play an essential role in intercellular communication in the central nervous system (1–3). The functional channels are oligomeric assemblies of 100-kDa subunits that can be assigned to one of three subfamilies: α-amino-3-hydroxy-5-methyl-4-isoxazole propionate (AMPA), *N*-methyl-D-aspartate, and kainate receptors (4). Following agonist binding, AMPA receptors induce depolarization of the postsynaptic membrane on a millisecond time scale (5), consistent with their role as the predominant mediators of fast excitatory synaptic transmission in the central nervous system (6). Depending on the agonist and receptor subtype involved, the channels then inactivate or desensitize (7–9), which is thought to be important physiologically for avoiding prolonged excitation and for responding to high frequency stimulation (10–13).

Mutagenesis experiments have located the GluR agonist-binding site in a domain distant from the ion channel gate (14), as has also been observed for the acetylcholine receptor (15). This implies that the presence of agonist in the binding site is communicated to the channel by means of conformational changes that propagate through the protein. This coupling of the state of the pore to the conformation of the agonist-binding site is reflected, for example, in different affinities for the resting and desensitized states of various receptors (the "binding-gating problem") (4, 16).

A ligand-binding domain identified within the GluR sequences has been extensively characterized (17–21). It can be expressed as a soluble fusion protein (S1S2) with a pharmacological profile similar to that of the intact solubilized receptor, at least for AMPA receptor subunits (17). Studies of S1S2-agonist binding can provide insight into conformational changes within the domain, decoupled from the subsequent rearrangements (*i.e.* channel gating and desensitization) that they drive in the intact molecule. These changes may reflect either stabilization of a pre-existing conformation or induction of a novel conformation, although we speak here of their being "driven" or "induced" by agonist binding for the sake of simplicity.

S1S2 is structurally related to the periplasmic binding proteins (PBP), bacterial proteins that bind metabolites in the cleft between two lobes. X-ray crystallography and solution scattering measurements on PBP reveal that the ligand first docks against lobe I in the open cleft and is then trapped by a dramatic cleft closure in the so-called "Venus flytrap" mechanism (22–27). It has been suggested that a similar lobe closure occurs in the ligand-binding domain of the GluR and that this closure acts as the trigger for channel gating and/or desensitization (19, 21, 28, 29). However, a dramatic lobe closure is not strictly required for ligand binding even among PBP family members, *e.g.* if the ligand can bridge the open cleft (30) or if oligomerization constrains the conformational flexibility (31). We suggest that both of these conditions may be fulfilled by GluR.

The crystallographic structure of an S1S2 domain core in complex with kainate has provided a detailed snapshot of its interaction with a ligand that induces unusually rapid (and weaker) desensitization in AMPA receptors compared with glutamate or AMPA. As a result, whole-cell currents induced by

* This work was supported by the Departments of Biophysics and Cell Physiology at the Max Planck Institute for Medical Research, European Union Fourth Framework Program in Biotechnology Grant BIO4-CT96-0589 (to D. R. M. and K. K.), and by the Academy of Finland (to K. K.). The costs of publication of this article were defrayed in part by the payment of page charges. This article must therefore be hereby marked "*advertisement*" in accordance with 18 U.S.C. Section 1734 solely to indicate this fact.

§ Present address: Inst. for Physiological Chemistry, Phillips-Universität Marburg, Karl-v.-Frisch-Str. 1, 35043 Marburg, Germany.

‖ To whom correspondence should be addressed. Tel.: 49-6221-486150; Fax: 49-6221-486437; E-mail: madden@mpimf-heidelberg.mpg.de.

[1] The abbreviations used are: GluR, glutamate receptor ion channel(s); AMPA, α-amino-3-hydroxy-5-methyl-4-isoxazole propionate; PBP, periplasmic binding protein(s); QBP, glutamine-binding protein.

kainate appear non-desensitizing (32). This x-ray structure has been interpreted as supporting a Venus flytrap mechanism (21). We have pursued a parallel biophysical comparison of the bound and free states of S1S2 to understand the nature and dynamics of the conformational changes induced by the binding of different ligands. In a first approach, we showed by solution scattering techniques that there is no reduction in the radius of gyration of S1S2 upon agonist binding, indicating that the magnitude of any conformational change in the domain must be considerably smaller than for the PBP (33). Circular dichroism measurements confirm that there are no significant changes in secondary structure content upon glutamate binding (34).

Here, we present an analysis of the affinity and kinetics of agonist binding to S1S2 from the AMPA receptor GluRD, monitored using an intrinsic tryptophan fluorescence signal and stopped-flow techniques. These data provide the first biophysical evidence that S1S2-agonist binding is a two-step process, in which docking is followed by isomerization. This isomerization represents the conversion of the free energy of agonist binding into mechanical changes by S1S2 alone, *i.e.* in the absence of load. Comparison with the (possibly distinct) S1S2 conformational changes that occur in the context of the intact receptor should ultimately provide insight into the mechanism by which agonist binding drives channel activation and desensitization. By analyzing the agonist binding kinetics of a panel of site-directed mutants, we have identified key side chains in the docking and locking steps. Our data also complement the recent finding that the phosphate-binding protein engages in rapid docking and subsequent slow cleft closure (35). This is in contrast to the earlier proposal of rapid isomerization for the arabinose-binding protein (36) and suggests that S1S2 and the PBP have similar kinetic profiles.

## EXPERIMENTAL PROCEDURES

*Protein Expression and Purification*—S1S2 from GluRD was prepared as described (17) with modifications (37). The panel of site-directed mutants has also been described (38).

*Fluorescence Titration*—All fluorescence spectra and titrations were measured with an SLM-AMINCO 8000 spectrofluorometer. The excitation band pass was 4 nm; the emission band pass was 8 nm; and the sample cell was maintained at 5 °C with a circulating water bath. All measurements were determined as the ratio between the fluorescence change of the sample and a reference cuvette filled with rhodamine to reduce the noise due to intensity fluctuations of the xenon lamp. The excitation wavelength was 280 nm for all measurements, and the fluorescence change of the titration measurements was followed at 336 nm. For the titration experiments, aliquots of 10 $\mu$l of concentrated ligand were added to a quartz cuvette containing 3 ml of protein (0.03–0.50 $\mu$M) in 10 mM $NaP_i$ (pH 7.3) and mixed continuously with a magnetic stirrer. For the titration measurements with AMPA, 100 mM KSCN, 2.5 mM $CaCl_2$, and 30 mM Tris (pH 7.2) was used for comparability with published measurements. Data points were collected every 3 s. For each ligand concentration, 20–25 data points were averaged. The fluorescence change was corrected for the dilution of the sample with ligand. The results were fitted by Equation 1,

$$F_i = F_0 + \Delta F_{max} \times \frac{(P_0 + L_0 + K_d) - \sqrt{(P_0 + L_0 + K_d)^2 - 4 \times P_0 \times L_0}}{2 \times P_0} \quad \text{(Eq. 1)}$$

where $F_i$ is the fluorescence observed after the $i$th addition of ligand, $F_0$ is the fluorescence of the free protein, $P_0$ is the total protein concentration, and $L_0$ is the total ligand concentration. Free parameters were the dissociation constant $K_d$ and the maximum fluorescence change in going from unbound to completely bound protein ($\Delta F_{max}$). Due to kainate absorbance at 280 nm at high concentrations, Equation 1 was modified to include an additional component linear in ligand concentration ($L_0$) for mutants E403Q and E706D, which had a very low affinity for kainate. Hill coefficients calculated for the binding reactions were between 0.9 and 1.1 (±0.05) for glutamate and kainate and slightly higher (1.0–1.5) for AMPA.

*Stopped-flow Kinetics*—Rapid kinetic measurements were performed in an SF-61 stopped-flow fluorometer (Hi-Tech Scientific). The excitation wavelength was 280 nm, and the fluorescence decrease was detected with a photomultiplier with a WG-320 filter (nominal cutoff of 320 nm). The dead time of the device was 1.0–1.5 ms. For glutamate and kainate, the kinetic measurements were performed in 10 mM $NaP_i$ (pH 7.3), and for AMPA, in 100 mM KSCN, 2.5 mM $CaCl_2$, and 30 mM Tris (pH 7.2), again for purposes of comparability with published data. Control experiments were also performed with AMPA in which 100 mM KCl replaced 100 mM KSCN. All measurements were carried out at 5 °C with a protein concentration between 0.05 and 5 $\mu$M. Pseudo first-order reaction conditions were employed (ligand concentration >5-fold higher than protein concentration). To improve the signal-to-noise ratio, five to seven individual traces for each ligand concentration were averaged. The measurements were repeated two to three times.

The reactions were monophasic for glutamate and kainate binding to all S1S2 variants; these time courses were fitted with a single exponential curve. For AMPA binding, a biphasic reaction was observed, of which one phase ($k_{obs} \cong 0.6–1.2\ s^{-1}$) was independent of added ligand and was thus apparently a mixing artifact caused by the presence of the chaotrope KSCN (monophasic reactions were observed when KCl replaced KSCN in the binding buffer). For AMPA concentrations above 10 $\mu$M, the contribution of the second phase could be ignored due to the rapid time course of the reactions, and the data were fitted with a single exponential curve. For lower concentrations, a biexponential fit was performed, but only the ligand-dependent time constant was considered.

Standard kinetic analysis was performed as described (39). For agonist/protein combinations showing a linear dependence of $k_{obs}$ on ligand concentration under pseudo first-order conditions, a one-step mechanism was assumed (see Equation 4 below). A least-squares linear fit was performed according to Equation 2,

$$k_{obs} = k_{off} + k_{on} \times \bar{L} \quad \text{(Eq. 2)}$$

where $\bar{L}$ is the concentration of free ligand. For agonist/protein combinations showing a nonlinear dependence of $k_{obs}$ on ligand concentration under pseudo first-order conditions, a two-step binding mechanism was assumed (see Equation 5 below) in which association is rapid compared with isomerization (see Equation 6 below). A nonlinear least-squares fit was performed according to Equation 3.

$$k_{obs} = k_{-2} + \frac{k_{+2} \times \bar{L}}{(K_{d1} + \bar{L})} \quad \text{(Eq. 3)}$$

*Modeling*—The interactions of glutamate with the S1S2 binding site (see Fig. 4*B*) were modeled by assuming that the glutamate atoms would adopt the same positions as corresponding atoms in kainate (*e.g.* glutamate $\alpha$-amino = kainate pyrrolidine nitrogen; $\alpha$-carboxylate = 2-carboxylate; $\delta$-carboxylate = 3-methyl carboxylate). Ligand interactions were plotted using the program LIGPLOT (40). Modeling of S1S2 side chain mutations was performed in O (41) using standard side chain rotamers (42).

## RESULTS

*S1S2-Ligand Binding Induces a Conformational Change*—The intrinsic fluorescence of S1S2 changed upon agonist binding (Fig. 1). Two facts suggest that Trp is the primary internal fluorophore, both for the intrinsic fluorescence and for the agonist-induced fluorescence change. The observed excitation maximum lies between 282 and 283 nm for the apo and holo forms of S1S2 and for the difference spectrum (emission monitored at 336 nm). Furthermore, using excitation wavelengths of 280 and 296 nm, similar emission spectra were obtained, although 296 nm excitation produced a weaker signal (at 336 nm, emission was ~16% of that seen at 280 nm; excitation at 290 nm yielded ~50%). None of the four S1S2 tryptophans is located in the immediate vicinity of the binding site (21), so this signal most likely reflects an isomerization process. Together with the nonlinear kinetic results presented below, this represents the first direct evidence that the S1S2 domain by itself undergoes a conformational change following ligand binding.

Kainate produces apparently non-desensitizing whole-cell currents at AMPA receptors due to its rapid desensitization kinetics (32), and it has thus been proposed that the kainate-

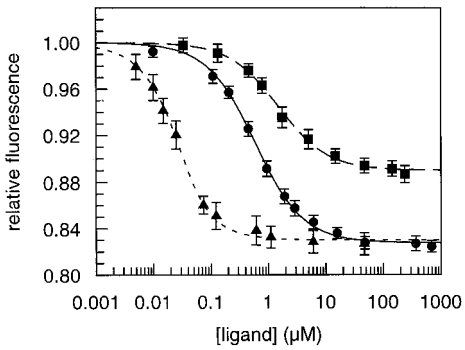


FIG. 1. **Fluorescence titrations of wild-type S1S2 binding to glutamate (*circles*), kainate (*squares*), and AMPA (*triangles*) at 5 °C, shown together with curves fit for a single binding site using Equation 1.** The affinities thus determined are shown in Table II. To accommodate the wide range of ligand concentrations, a semilog plot was used.

bound x-ray structure reflects a non-desensitized, activated state intermediate between the resting and desensitized states (21). Here, we observed that the maximum fluorescence change ($\Delta F_{max}$, Equation 1) observed in the presence of saturating concentrations of agonist was smaller for kainate (−10.8 ± 3.8%) than for glutamate (−19.0 ± 1.2%) or AMPA (−17.0 ± 1.3%). Although we cannot assign the conformational changes in S1S2 to functional states of the intact receptor, it is possible that the more rapid and partial desensitization induced by kainate reflects smaller induced conformational changes in the domain.

Since we do not know which tryptophan residue(s) contribute to the signal, it is not possible to interpret the fluorescence change directly in structural terms. However, the fluorescence change permitted us to measure the kinetics of protein-ligand association following rapid mixing. In addition, comparison of the kinetics of wild-type S1S2 and site-directed mutants enabled us to assess structural changes associated with the initial steps of ligand binding.

The kinetic behavior of protein-agonist binding was monophasic, rapid, and concentration-dependent over a wide range of agonist concentrations (Fig. 2). Under pseudo first-order conditions, the apparent rate constants ($k_{obs}$) for AMPA and glutamate showed a linear dependence on ligand concentration (Fig. 2*D*), yielding estimates (Table I) for overall association ($k_{on}$) and dissociation ($k_{off}$) rate constants analogous to values determined for a number of PBP for a one-step binding mechanism (36, 43, 44) (Equation 4),

$$P + L \underset{k_{off}}{\overset{k_{on}}{\rightleftharpoons}} PL \qquad \text{(Eq. 4)}$$

where P is S1S2 and L is agonist.

The rate constants thus obtained for glutamate are similar to those of PBP specific for various amino acids and sugars, with a rapid, but not necessarily diffusion-limited, $k_{on}$ on the order of $10^7$ to $10^8$ $M^{-1}$ $s^{-1}$ (here, $1.6 \times 10^7$ $M^{-1}$ $s^{-1}$) and a slow $k_{off}$ on the order of 1–10 $s^{-1}$ (here, 7.6 $s^{-1}$). This slow glutamate dissociation rate constant also agrees broadly with values obtained by modeling electrophysiological data: rate constants for quisqualate and domoate dissociation from AMPA receptors have been estimated at 30–37 $s^{-1}$ (45), and those for glycine dissociation from *N*-methyl-D-aspartate receptors at 0.3–1.3 $s^{-1}$ (46). The dissociation rate constant for AMPA is significantly slower than that for glutamate: 0.06 $s^{-1}$. This is also consistent with an estimate of 0.032 $s^{-1}$ for AMPA dissociation from rat brain membranes (47). When KSCN was replaced by KCl in the AMPA binding buffer, a linear concentration dependence of $k_{obs}$ was also observed; consistent with observations on intact receptors, the main effect of KSCN is to stabilize the ligand-bound form, *i.e.* to reduce $k_{off}$ (34, 47).

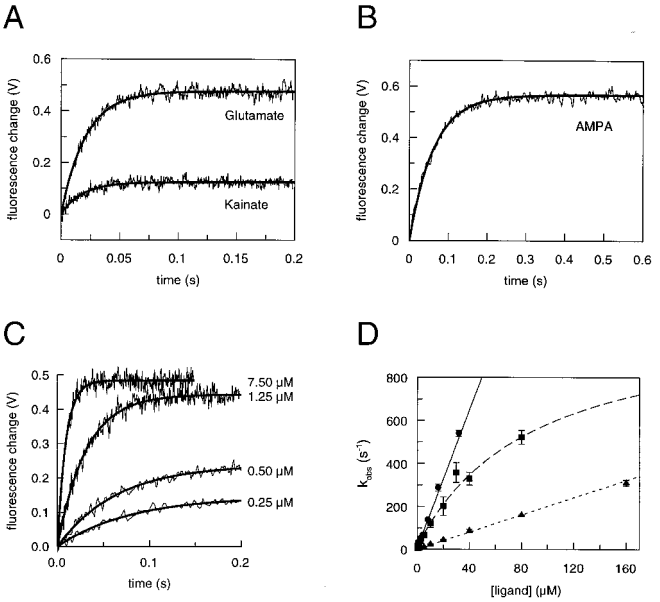


FIG. 2. **Kinetics of wild-type S1S2-agonist binding.** *A* and *B*, stopped-flow time courses obtained for glutamate (2.5 μM) and kainate (3 μM) and for AMPA (10 μM) binding, respectively, to wild-type S1S2 under pseudo first-order conditions at 5 °C. *C*, stopped-flow time courses obtained for glutamate binding to wild-type S1S2 under pseudo first-order conditions at 5 °C at four different glutamate concentrations. Single exponential fits are superimposed on the experimental data. *D*, concentration dependence of the pseudo first-order rate constants for association of AMPA (*triangles*), kainate (*squares*), and glutamate (*circles*) with wild-type S1S2 as determined by stopped-flow measurements. The *curves* show linear fits for glutamate (*solid line*) and AMPA (*finely dashed line*) binding and a hyperbolic fit for kainate binding (*coarsely dashed line*). The concentration dependence of $k_{obs}$ for AMPA remains linear to the resolution limit of our apparatus (~600 $s^{-1}$ at 300 μM AMPA).

Unfortunately, a more detailed comparison of the kinetics of S1S2- and GluR-ligand binding is precluded by the paucity of experimental results on the intact molecule. This is due to limitations in the speed of agonist application in electrophysiological experiments and to difficulties expressing and purifying sufficient quantities of GluR for biochemical measurements. Flash photolysis techniques (48) and the large-scale expression of recombinant intact GluR[2] may permit more detailed comparison in the future.

Unlike the AMPA and glutamate values, the pseudo first-order rate constants for kainate show a hyperbolic dependence on ligand concentration (Fig. 2*D*). This is not consistent with a one-step binding mechanism, nor is it consistent with a Venus flytrap mechanism in which the cleft closure step is faster than the initial binding step, as has been proposed for the arabinose-binding protein (36). It would, however, be consistent with a two-step dock/lock mechanism (Equation 5),

$$P + L \underset{k_{-1}}{\overset{k_{+1}}{\rightleftharpoons}} PL \underset{k_{-2}}{\overset{k_{+2}}{\rightleftharpoons}} P^*L \qquad \text{(Eq. 5)}$$

in which P is S1S2 in its unbound conformation, P* is S1S2 following isomerization, and the transition from P to P* produces the fluorescence signal, provided that binding is more rapid than isomerization, *i.e.* (Equation 6),

$$k_{+1}(\bar{P} + \bar{L}) + k_{-1} \gg k_{+2} + k_{-2} \qquad \text{(Eq. 6)}$$

[2] M. Safferling, K. Keinänen, and D. R. Madden, unpublished data.

TABLE I
*Kinetic parameters of agonist binding to S1S2*

| Agonist/construct | $K_{d1}$ [a] | $k_{+2}$ [a] | $k_{-2}$ [a] ≡ $k_{off}$ [b] | $k_{on}$ [b] | Calculated $K_d$ [c] |
|---|---|---|---|---|---|
| | $\mu M$ | $s^{-1}$ | $s^{-1}$ | $\mu M^{-1}\ s^{-1}$ | $\mu M$ |
| Glutamate | | | | | |
| Wild-type | | | 7.6 ± 0.8 | 16.0 ± 0.9 | 0.48 ± 0.06 |
| E403D[d] | 122.9 ± 48.9 | 1247.9 ± 363.5 | 23.6 ± 4.1 | | 2.3 ± 1.2 |
| E403Q | 403.6 ± 70.7 | 850.2 ± 103.5 | 35.1 ± 1.8 | | 16.0 ± 3.4 |
| K450H | 151.8 ± 109.0 | 1519.7 ± 848.7 | 40.9 ± 2.8 | | 4.0 ± 3.6 |
| Y451F | 79.0 ± 36.8 | 1006.8 ± 289.0 | 72.9 ± 9.0 | | 5.3 ± 2.9 |
| E706D | 113.9 ± 63.8 | 809.9 ± 174.6 | 136.8 ± 31.6 | | 16.5 ± 10.3 |
| E706A | NM[e] | NM | NM | NM | NM |
| Kainate | | | | | |
| Wild-type | 90.2 ± 3.6 | 1082.5 ± 189.2 | 14.5 ± 1.5 | | 1.16 ± 0.38 |
| E403D | 61.9 ± 49.5 | 855.3 ± 443.6 | 8.2 ± 15.4 | | 0.59 ± 1.21 |
| E403Q | 807.1 ± 206.7 | 847.6 ± 154.5 | 36.8 ± 2.3 | | 33.6 ± 10.6 |
| K450H | | | 6.5 ± 0.5 | 8.6 ± 0.2 | 0.76 ± 0.06 |
| Y451F | 323.8 ± 37.5 | 1845.5 ± 175.2 | 26.3 ± 0.9 | | 4.5 ± 0.7 |
| E706D | NM | NM | NM | NM | NM |
| E706A | ND | ND | ND | ND | ND |
| AMPA | | | | | |
| Wild-type | | | 0.06 ± 0.06 | 2.0 ± 0.02 | 0.03 ± 0.03 |
| E403D | | | 0.20 ± 0.07 | 2.5 ± 0.1 | 0.08 ± 0.03 |
| E403Q | | | 0.08 ± 0.05 | 2.7 ± 0.1 | 0.03 ± 0.02 |
| K450H | | | 0.08 ± 0.17 | 1.6 ± 0.1 | 0.06 ± 0.11 |
| Y451F | | | 0.31 ± 0.03 | 1.9 ± 0.0 | 0.16 ± 0.02 |
| E706D | | | 0.41 ± 0.26 | 2.6 ± 0.1 | 0.16 ± 0.10 |
| E706A | | | 121.3 ± 9.7 | 0.24 ± 0.04 | 501.3 ± 92.7 |

[a] $K_{d1}$, $k_{+2}$, and $k_{-2}$ were determined only for nonlinear experimental data, from the hyperbolic least-squares fits shown in Figs. 2 and 3.
[b] $k_{on}$ and $k_{off}$ were determined only for linear experimental data, from the slope and $y$ intercept, respectively, of the least-squares linear fits shown in Figs. 2 and 3.
[c] The initial slope of a hyperbolic curve is given by $k_{+2}/K_{d1}$. Thus, assuming a two-step binding mechanism as described by Equation 5, $k_{off}/k_{on} = K_{d1} \times K_{d2}$.
[d] See Footnote *a* concerning residue numbering in Table II.
[e] NM, not measurable; ND, not determined.

where $\bar{P}$ and $\bar{L}$ are the equilibrium concentrations of free S1S2 and agonist, respectively (39). In this case, we can estimate the equilibrium dissociation constant for docking ($K_{d1}$) and the forward and backward isomerization rate constants ($k_{+2}$ and $k_{-2}$) for the reaction with kainate (Table I). Such slow isomerization was recently demonstrated for the phosphate-binding protein (35). The hyperbolic concentration dependence of $k_{obs}$ for S1S2 also supports the observation that the reporter Trp residue(s) must be distant from the binding site and therefore sensitive to the isomerization, rather than the docking, step.

Consistent with slow isomerization in S1S2, kinetic measurements on hippocampal neurons using caged kainate reveal that channel opening occurs more slowly than agonist binding (48). These measurements also yielded forward and backward rate constants of activation for intact AMPA receptors of 5000 and 640 $s^{-1}$, respectively, faster than the values detected here for S1S2 (Table I). This difference may indicate that free S1S2 is passing beyond a state corresponding to the open state to one corresponding to the desensitized state. Alternatively, coupling of the S1S2 changes to other conformational changes occurring in the intact receptor may speed these processes *in vivo*.

*Residual Affinity of $Arg^{486}$ and $Glu^{706}$ Mutants*—To further characterize the ligand-binding mechanism and to attempt to understand the different shapes of the kainate (hyperbolic) and glutamate (linear) $k_{obs}$ binding curves, we also studied a panel of 10 S1S2 site-directed mutants (Table II; see note on residue numbering) (38). The selection of candidate residues was greatly facilitated by extensive preceding mutagenesis of the S1S2 domain, allowing us to focus on residues known to affect binding affinity and/or channel gating properties (38). Fluorescence titrations were performed on the mutants (Table II) to select suitable mutants for kinetic analysis and to provide a reference affinity measurement for comparison with that calculated from the kinetic data. All of the mutants tested showed an intrinsic fluorescence change upon agonist binding, with the exception of E706Q, for which no fluorescence change could be detected up to 0.4 mM AMPA or 23 mM glutamate. It is possible that E706Q retains a residual affinity for agonists, but fails to undergo isomerization and therefore exhibits no fluorescence change upon binding. E706Q was also poorly expressed in several experiments, which may indicate that this mutation fundamentally destabilizes the protein. The fluorescence titration curves for all three agonists binding wild-type S1S2 could be fit with a hyperbolic curve for a single binding site (Fig. 1). The same was true for all S1S2 mutants, with the exception of the very weak kainate binders E403Q and E706Q, which required correction for kainate absorbance at 280 nm (data not shown).

Strikingly, the greater sensitivity of this technique compared with filter binding made it possible to detect weak binding of both AMPA and glutamate to the mutant R486K, which has been reported to abrogate both agonist binding and channel function (28, 38, 49–52) and which has been termed an "absolute requirement for the acquisition of ligand-binding activity" by GluRA (53). The affinity for glutamate was weakened by only 900-fold, whereas that for AMPA was reduced by >20,000-fold (Table II). The mutation E706A, for which neither binding nor channel activation has been detected previously (29, 38, 50), also was shown to have a weak residual affinity for glutamate and AMPA (Table II), reduced 40,000- and 25,000-fold, respectively. In the kainate·S1S2 core complex, $Arg^{486}$ and $Glu^{706}$ are responsible for binding the homologs of the α-carboxyl and α-amino moieties shared by most GluR agonists (21), as had been proposed based on their importance for ligand binding affinity (38). To further characterize the importance of the ligand's α-amino group, we also assessed the affinity of wild-type S1S2 for glutaric acid, which is identical to glutamate except for the absence of an α-amino group; using fluorescence titration, no binding could be detected up to a ligand concentration of 7.8 mM.

The effects of the other mutants on ligand affinities did not show significant deviations from those observed using filter

TABLE II
*Equilibrium dissociation constants of S1S2 mutants*
Equilibrium constants were determined by least-squares fits to fluorescence titration data (see Equation 1 under "Experimental Procedures").

| Construct | AMPA | Glutamate | Kainate |
|---|---|---|---|
| | *nM* | *μM* | *μM* |
| S1S2 | 8.8 ± 0.5 | 0.55 ± 0.03 | 1.45 ± 0.08 |
| S1S2 E403D[a] | 5.6 ± 1.1 | 2.75 ± 0.28 | 3.67 ± 0.22 |
| S1S2 E403Q | 6.6 ± 2.5 | 15.45 ± 0.95 | 34.91 ± 14.97 |
| S1S2 K450H | 37.1 ± 16.7 | 2.71 ± 0.01 | 1.39 ± 0.40 |
| S1S2 K450A | 26.7 ± 6.9 | 1.02 ± 0.01 | 1.57 ± 0.15 |
| S1S2 K450R | 7.7 ± 2.8 | 0.59 ± 0.02 | 1.03 ± 0.09 |
| S1S2 Y451F | 129.9 ± 30.3 | 6.80 ± 0.56 | 3.33 ± 0.07 |
| S1S2 R486K | (207.2 ± 71.5) × $10^{+3}$ | 476.4 ± 187.3 | ND[b] |
| S1S2 E706D | 7.5 ± 5.7 | 31.29 ± 4.56 | (3.48 ± 1.67) × $10^{+3}$ |
| S1S2 E706A | (223.1 ± 24.1) × $10^{+3}$ | (22.9 ± 5.5) × $10^{+3}$ | ND |
| S1S2 E706Q | NB | NB | ND |

[a] The numbering scheme used here refers to the mature GluRD sequence. Residue numbers are smaller by 21 than those reported by Lampinen *et al.* (38). Residue numbers in mature GluRB (21) are smaller by 1 than those in GluRD. For example, $Glu^{706}$ in GluRD corresponds to $Glu^{705}$ in GluRB and $Glu^{727}$ using the system of Lampinen *et al.* (38).
[b] ND, not determined; NB, no binding.

binding studies (38), although in some cases, detailed comparisons were limited by large standard deviations. In two cases, apparent differences were clearly affected by technical limitations. Y451F showed a clearly reduced affinity for glutamate by fluorescence titration (Table II), whereas competition binding data revealed no change (38). Although reproducible, the filter binding data may have been compromised by the 15-fold reduced affinity of Y451F for the reporter ligand AMPA and/or by an increase in the dissociation constant for AMPA (nearly 8-fold). The affinity of AMPA for mutant E706D appeared to increase significantly according to filter binding studies, whereas fluorescence titration revealed no obvious shift. Given such tight binding, the equilibrium dissociation constant calculated by fluorescence titration is necessarily imprecise (since the minimum protein concentration required to obtain a signal is large relative to $K_d$) and represents only an upper limit. In this case, the filter binding data are likely to be more accurate due to the much lower protein concentration required. In general, however, the fluorescence data are more accurate than those determined by filter binding techniques for glutamate and kainate. Overall, the fluorescence data also reproduce the results of mutagenesis studies on agonist binding and electrophysiology (*e.g.* Refs. 29, 49, and 50).

*Mutants Isomerize Slowly after Binding Glutamate*—Stopped-flow measurements were performed with seven mutants, each of which had shown an altered ligand affinity profile as judged by fluorescence titration. Of these, kinetics could not be followed by the stopped-flow technique for R486K binding to any ligand, for E706A binding to glutamate or kainate, or for E706D binding to kainate, presumably due to the extreme destabilization of the resulting complexes (see below). Six mutants, affecting four side chains, proved suitable for kinetic analysis (Fig. 3 and Table I). As for the wild-type protein, each mutant showed a single relevant, concentration-dependent time constant of fluorescence change per agonist concentration. As would be expected, the affinities calculated from the measured kinetic parameters (Table I) are in good agreement with those measured by fluorescence titration (Table II). Differences were observed for E403D binding to kainate and AMPA, but these are most likely due to technical difficulties in the kinetic measurement of extremely small $k_{-2}$ values, which are reflected in the large standard deviations.

For all six mutants, the concentration dependence of the pseudo first-order rate constant was linear for AMPA, as it had been for the wild-type protein. A hyperbolic dependence was observed for three of four mutants whose binding to kainate could be followed kinetically, again consistent with the wild-type observations; K450H showed a linear dependence suggestive of a sharp increase in $k_{+2}$. Unlike the wild-type protein, all five mutants whose binding to glutamate could be followed (E403D, E403Q, K450H, Y451F, and E706D) exhibited a nonlinear dependence of the pseudo first-order rate constant on glutamate concentration. This strongly suggests that these mutants bind glutamate in a two-step process, in which a rapid "docking" of protein and ligand is followed by a slower "locking" isomerization. In addition, this analysis permitted us to identify the contribution of individual side chains to each process.

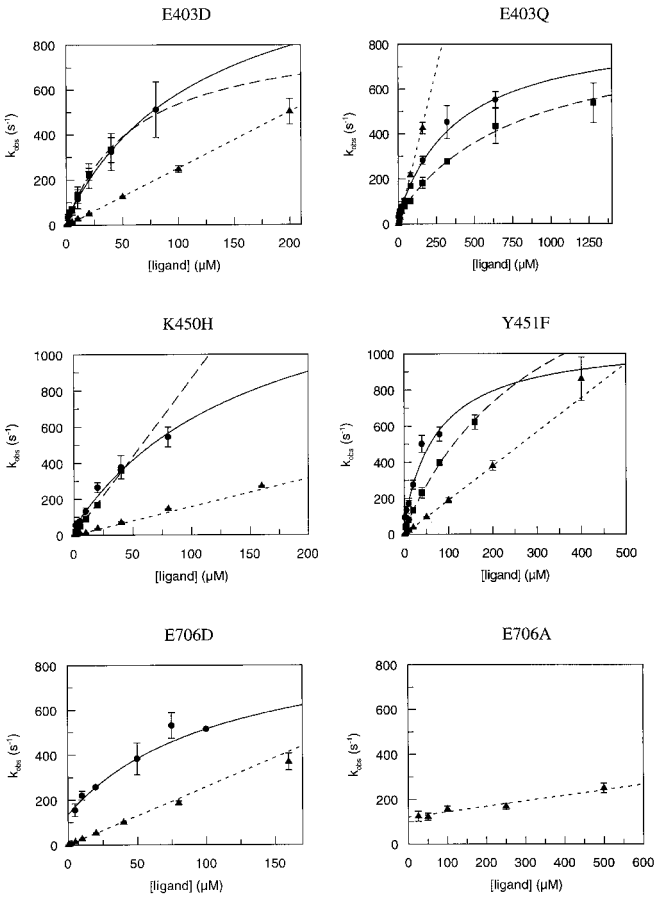


FIG. 3. **Concentration dependence of the pseudo first-order rate constants for agonist binding to S1S2 mutants.** The symbols and fitted curves are as described in the legend to Fig. 1*B*. Note the different ranges for ligand concentrations necessary to resolve the data for different mutants.

*Docking*—Mutations in two side chains, $Glu^{403}$ and $Tyr^{451}$,

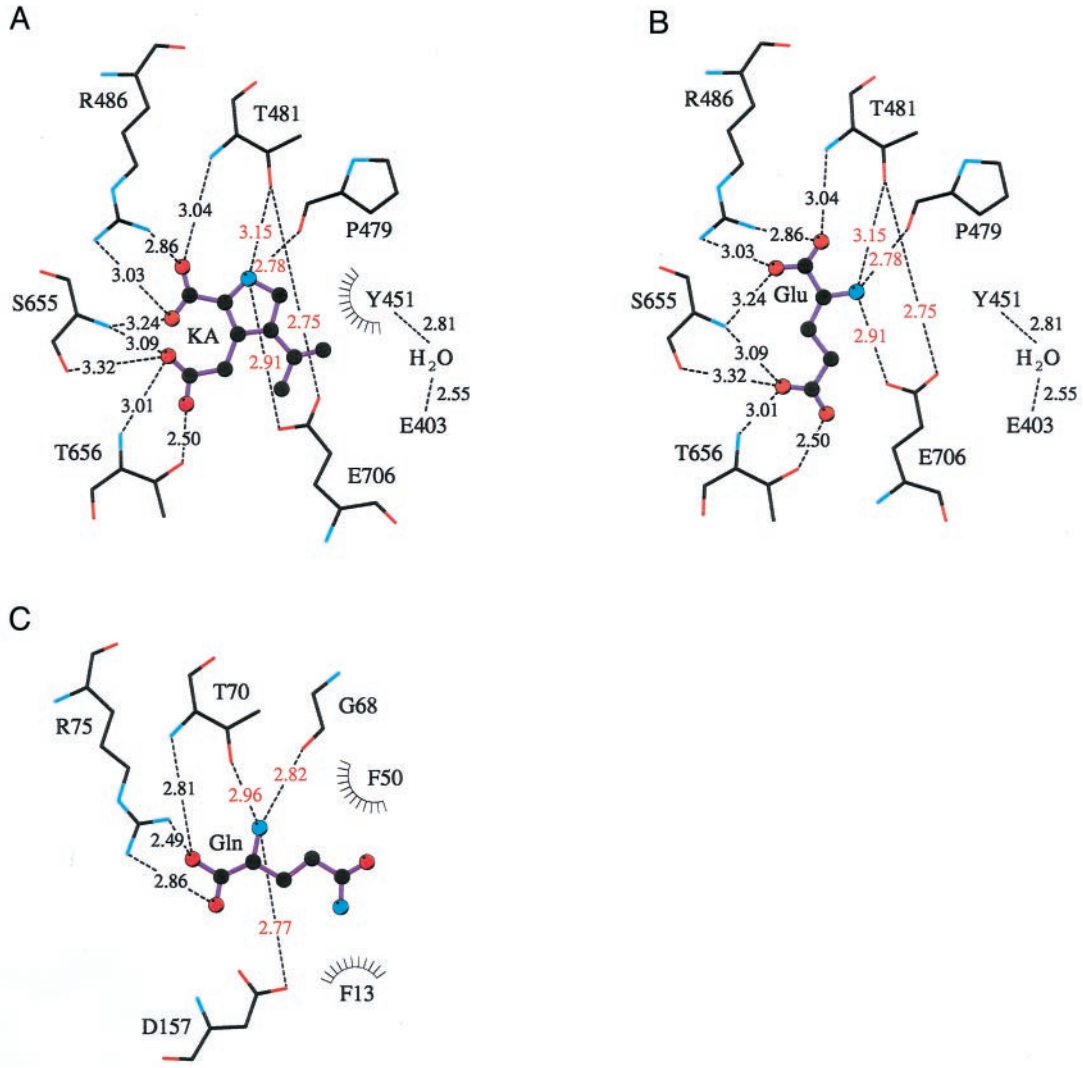


FIG. 4. **Schematic representation of selected hydrogen bond and hydrophobic interactions between ligand and binding protein for the S1S2 core domain with kainate (21) (*A*), a model of the S1S2 core domain with glutamate (*B*), and QBP with glutamine (58) (C).** The ligand is shown as a ball-and-stick figure. Binding protein residues are shown as stick figures with bonds colored by atom type: *black*, carbon; *red*, oxygen; and *blue*, nitrogen. Residues from lobe I are clustered above and to the right of the ligands ($Arg^{486}$, $Thr^{481}$, $Pro^{479}$, $Tyr^{451}$, and $Glu^{403}$ for S1S2; $Arg^{75}$, $Thr^{70}$, $Gly^{68}$, $Phe^{13}$, and $Phe^{50}$ for QBP). Residues from lobe II are clustered below and to the left of the ligand ($Glu^{706}$, $Thr^{656}$, and $Ser^{655}$ for S1S2; $Asp^{157}$ for QBP). The three-way hydrogen-bonding network discussed under "Results" is highlighted (*red* bond distances). Although the binding site is distorted by the projection algorithm, the relative orientations of the ligands approximately reflect those found in three dimensions, *e.g.* by superposition of secondary structure elements of lobe I. The hinge axis runs approximately horizontal.

clearly affected $K_{d1}$, *i.e.* the affinity of the binding site for ligand in the initial, docking step (Table I). Both are located in lobe I, suggesting that the initial complex is formed here, in analogy to the PBP (26). For kainate, E403Q and Y451F both increased $K_{d1}$ relative to the wild type, whereas E403D did not. For glutamate, $K_{d1}$ could not be determined for wild-type S1S2. However, as observed for kainate, E403Q increased $K_{d1}$ relative to E403D. Y451F did not.

In the structure of the S1S2 core bound to kainate, $Glu^{403}$ does not contact kainate directly. Instead, it forms a hydrogen bond via a water molecule to $Tyr^{451}$ (Fig. 4*A*) (21). Working from this structure, we found that a standard rotamer of $Asp^{403}$ could form a direct hydrogen bond to $Tyr^{451}$ in its wild-type conformation, possibly accounting for the lack of disruption observed in E403D *versus* wild-type binding of kainate. Thus, the E403D value may act as a surrogate for the $K_{d1}$ for wild-type binding of glutamate, which cannot be measured directly. However, $Gln^{403}$, which disrupted kainate docking relative to the wild type and glutamate docking relative to E403D (Table I), should be able to form the same hydrogen-bonding network with $Tyr^{451}$ as $Glu^{403}$. Thus, it appears that for this residue, the negative charge, rather than the water-mediated hydrogen bond to $Tyr^{451}$, may be important for the docking step. Curiously, E403A shows wild-type affinity for AMPA and glutamate (38); however, in the absence of kinetic measurements, it is possible that compensating changes in the locking equilibrium mask changes in docking affinity or *vice versa*.

$Tyr^{451}$ engages in van der Waals interactions with the isopropenyl group of bound kainate (Fig. 4*A*). If glutamate binds S1S2 with its carboxyl and amino groups in the same positions as those of kainate, then there would be no interaction between glutamate and $Tyr^{451}$ (Fig. 4*B*). Consistent with this model, Y451F increased the $K_{d1}$ for kainate, but probably not that for glutamate; the indirect hydrogen bond to $Glu^{403}$ presumably constrains $Tyr^{451}$ to a conformation that does not interfere with the volume occupied by bound kainate. Cast free, $Phe^{451}$ could transiently block the kainate, but not the smaller glutamate-binding site. In any case, it is unlikely that $Tyr^{451}$ contacts bound glutamate directly, which would require a substantial cleft closure or side chain rearrangement relative to the

kainate structure (21).

The linear $k_{obs}$ *versus* ligand concentration curves for AMPA lie below and to the right of hyperbolic curves for kainate binding to wild-type S1S2 and for glutamate and kainate binding to all mutants but one (Fig. 3). Since no curvature was detected for AMPA, it appears that the docking affinity $K_{d1}$ of AMPA is substantially weaker than those of glutamate and kainate. For E403Q binding, the AMPA line lies above the other curves; in this case and in the comparison of glutamate and AMPA binding by wild-type S1S2, no information is available about relative $K_{d1}$ values. The rate constants reveal that high affinity binding of AMPA (Table II; $K_d$ 60-fold tighter than for glutamate) is due instead to the exceptional stability of the complex once formed. The overall dissociation rate constant ($k_{off}$) is 190-fold slower than that for glutamate (Table I). This may be due to the expected ability of the side chain isoxazole moiety to form more extensive interactions with lobe II than kainate or glutamate (21). The high stability of the AMPA·S1S2 complex is consistent with its suitability for filter binding experiments.

*Locking*—Two $Glu^{706}$ mutants, E706D and E706A, strongly affected the backward rate constant of isomerization ($k_{-2}$), *i.e.* the speed of "unlocking", without apparently affecting docking affinity. For AMPA, $k_{-2}$ was increased 7-fold in E706D and >2000-fold in E706A (Table I). For glutamate, $k_{-2}$ was increased 18-fold in E706D. Agonist binding could not be followed by stopped-flow techniques for glutamate binding to E706A and for kainate binding to both mutants, even though fluorescence titration measurements revealed (weak) ligand binding for glutamate to E706A and for kainate to E706D. A likely explanation is that the weak affinity also reflects a sharp increase in $k_{-2}$, which is the minimum rate that can be observed: if $k_{-2} \gg 500\ s^{-1}$, the time course will be inaccessible to our stopped-flow device since $k_{obs} \geq k_{-2}$ (Equation 3). E706Q, for which no binding could be detected even by titration experiments, may have an even higher value for $k_{-2}$. Alternatively, it may not isomerize upon agonist binding, so no fluorescence signal can be detected. In the one $Glu^{706}$ mutant for which $K_{d1}$ and $k_{+2}$ could be estimated (glutamate binding to E706D), neither the equilibrium dissociation constant for docking nor the forward isomerization rate constant was significantly destabilized relative to other mutants. Thus, it appears that $Glu^{706}$ is essential for stabilizing the "locked" conformation, rather than for docking. In addition, it appears that a negative charge is essential.

In complex with kainate, $Glu^{706}$ binds the pyrrolidine nitrogen (21), which presumably corresponds to the α-amino group in glutamate. The amino group also forms hydrogen bonds to the carbonyl group of $Pro^{479}$ and to the side chain of $Thr^{481}$, which in turn is hydrogen-bonded to $Glu^{706}$ (Fig. 4, *A* and *B*; hydrogen bonding distances shown in *red*). The three-way hydrogen-bonding network of $Thr^{481}$, $Glu^{706}$, and the agonist amino group, in which each component binds the other two, thus knits together the two lobes of the protein and the agonist. The nearly tetrahedral geometry of the hydrogen bonds formed by the ligand's nitrogen atom is well suited to the α-amino moiety of the physiological ligand.

$Lys^{450}$ may play a secondary role in the locking process. In the kainate structure, $Lys^{450}$ is located at the periphery of the binding site, does not interact directly with the agonist, and is distant from any potential "hinge" positions. However, it has been proposed that following further cleft closure, $Lys^{450}$ could stabilize glutamate binding by reaching across the lip of the cleft to bind $Asp^{652}$ or $Ser^{653}$. Thus, it should be a locking residue for glutamate, but not kainate (21). It is therefore surprising that the K450H mutation affected both $k_{+2}$ and $k_{-2}$ for kainate (Table I). The forward rate constant ($k_{+2}$) appeared to have increased significantly relative to the wild type since this mutant showed a linear dependence of $k_{obs}$ on ligand concentration for kainate, whereas the wild-type dependence was hyperbolic (Figs. 2*D* and 3; see "Discussion"). The backward rate constant ($k_{-2}$) actually decreased, *i.e.* the K450H substitution stabilized the locked conformation of the kainate complex. In contrast to the unexpected results with kainate, the effect of the mutation K450H on glutamate binding is consistent with a proposed role in stabilizing the locked conformation of the glutamate complex (21). K450H increased $k_{-2}$ for glutamate 5-fold and apparently decreased $k_{+2}$ since the linear $k_{obs}$ dependence of the wild type was replaced by a nonlinear dependence in the mutant (Figs. 2*D* and 3; see "Discussion").

## DISCUSSION

*The Motor That Drives GluR*—Interpreted in terms of the structure of the kainate-bound S1S2 core (21), these data suggest a first picture of the sequence of interactions between agonist and the GluR ligand-binding domain. Agonists dock to lobe I of S1S2 adjacent to a ridge formed by side chains $Glu^{403}$ and $Tyr^{451}$. Following relatively rapid docking, the binding site then undergoes a slower isomerization that leads to formation of a stable high affinity complex. A three-way hydrogen-bonding network involving the agonist amino moiety and the side chains $Thr^{481}$ on lobe I and $Glu^{706}$ on lobe II appears to play a key role in locking the agonist in.

Of course, our data apply to the S1S2 ligand-binding domain alone, acting outside the context of the intact receptor. In the absence of intact GluR structures, it is impossible to establish whether its agonist-bound conformation corresponds closely to that of the domain in the open or desensitized GluR (or neither) since these states have meaning only for a functional ion channel. The high affinity of isolated S1S2 for agonists is reminiscent of values reported for inhibition constants rather than $EC_{50}$ values (4), suggesting that agonist-bound ("holo-") S1S2 may be more similar to the desensitized state than to the open state of GluR. However, holo-S1S2 may instead approximate the open state. In this case, the discrepancy between the $K_d$ values of S1S2 and the $EC_{50}$ values of GluR would reflect S1S2's uncoupling of agonist binding from the energetically unfavorable process of channel opening.

Given this ambiguity, we prefer not to attempt to assign holo-S1S2 to a specific functional state. Instead, we wish to emphasize that the motions undergone by S1S2 on its own represent the fundamental molecular process that converts agonist-binding energy into conformational changes. These changes are presumably harnessed to drive channel gating and/or subsequent desensitization in the intact receptor.

Despite this ambiguity, $Glu^{706}$ and $Thr^{481}$ may play an important role in channel gating. Mutations to alanine of the $Glu^{706}$ homologs in NR2A ($Asp^{731}$) and NR2B ($Asp^{732}$) and of the $Thr^{481}$ homolog in GluRA ($Thr^{476}$) abolish channel activity (29, 54). Thus, we propose that recruitment of $Glu^{706}$ and $Thr^{481}$ into a hydrogen-bonding network with agonist could well be a key step in channel gating. On the other hand or in addition, it is possible that these mutations operate indirectly on the $EC_{50}$ values, via changes in the desensitized state(s) of the molecule. A test of these alternatives would be provided by an analysis of antagonist binding to appropriately mutated intact GluR channels. Due to UV absorption by the antagonist compounds, fluorescence binding studies are, however, not feasible.

The foregoing proposal does not exclude the possibility that the holo-S1S2 end state may have similarity to the desensitized conformation. This is suggested by two observations. First, the

kinetics we observed for S1S2 binding of kainate are slower than those determined by flash photolysis for kainate activation of GluR (48). Second, the rapid and partial desensitization induced by kainate (32) corresponds qualitatively to the observation that kainate induces a smaller fluorescence change in S1S2 than do glutamate and AMPA. As mentioned above, however, a detailed comparison of S1S2 and GluR structures in defined states will ultimately be required to determine the functional correlates of the apo and holo forms of S1S2.

*Comparison of PBP and S1S2 Kinetics*—Qualitatively, two types of kinetic behavior were observed for the binding of agonists to S1S2. Wild-type S1S2 bound AMPA and glutamate with an observed rate constant that increased linearly with increasing agonist concentration. The same linear dependence was observed for AMPA binding to all S1S2 mutants studied here and for kainate binding to K450H. In contrast, a hyperbolic dependence of $k_{obs}$ on agonist concentration was observed for glutamate binding to all S1S2 mutants studied and for kainate binding to wild-type and all mutant S1S2 molecules but one.

What explains the different dependence of $k_{obs}$ on agonist concentration? We propose that isomerization is slower than binding for all three agonists binding to all S1S2 molecules, but that large $k_{+2}$ values make it impossible to detect hyperbolic behavior in some cases due to the limited temporal resolution of the stopped-flow apparatus. Significant departure from linearity is observed only for values of $k_{obs}$ approaching $(2k_{-2} + k_{+2})/2$. Since the resolution of our stopped-flow device is roughly 500 $s^{-1}$, saturation behavior is inaccessible for reactions with $k_{+2} \gg 1000\ s^{-1}$, and the smallest value of $k_{+2}$ we detected was 850 $s^{-1}$ (Table I). If the values for glutamate binding of wild-type S1S2 or for kainate binding of K450H were only severalfold higher, then our experiments could measure only the initial, linear phase of the hyperbolic curve. Unfortunately, attempts to surmount the kinetic limitation for S1S2 using faster pressure- or temperature-jump experiments were not technically feasible (34).[3]

If this hypothesis is correct, one effect of the mutations would be to reduce $k_{+2}$ sufficiently to bring the saturation regime within experimental reach, say by an order of magnitude or less. This is consistent with the relatively modest shifts in $k_{+2}$ seen for kainate binding (Table I). Calculations with $K_{d1} = 1$ mM and $k_{+2} = 2 \times 10^4\ s^{-1}$ ($k_{-2} = 7.6\ s^{-1}$) yield kinetic behavior consistent with that shown in Fig. 2*D* for glutamate binding to wild-type S1S2. Assuming additionally that $k_{+1}$ is $\geq 10^8\ M^{-1}\ s^{-1}$, locking would indeed be slower than docking for wild-type S1S2 binding of glutamate at physiological concentrations.

The same technical limitation most likely also affected earlier measurements of PBP-ligand binding kinetics. A linear concentration dependence of $k_{obs}$ for the arabinose-binding protein had been interpreted as showing that isomerization is faster than initial docking (36). However, recent stopped-flow measurements on a Trp mutant of the phosphate-binding protein revealed a hyperbolic dependence of $k_{obs}$; the mutant protein was shown to have wild-type phosphate affinity, and the introduced reporter Trp side chain was shown crystallographically to be distant from the bound phosphate (35). These data were interpreted in terms of nearly diffusion-limited docking and relatively slow isomerization. Slow isomerization has also been detected for the dicarboxylate-binding protein DctP, although this protein preferentially adopts the closed conformation in the absence of ligand and therefore must additionally open *before* binding ligand, in contrast to the other PBP studied (55).

It seems likely that the linear concentration dependence of $k_{obs}$ seen for the arabinose-binding protein simply represents the initial (linear) phase of a hyperbolic curve, as it probably does when observed for S1S2. This interpretation is also consistent with the fact that the maximal ligand concentrations used in kinetic studies of the arabinose-binding protein (100 $\mu$M) probably did not approach $K_{d1}$, the point at which significant curvature would be observed (36, 44). Electron density peaks from ligands soaked into crystals of the open form of the leucine/isoleucine/valine-binding protein did not show saturation at concentrations as high as 10–50 mM, *i.e.* >2 orders of magnitude higher (56). According to this proposal, all PBP would share a common kinetic motif with the GluR: rapid docking followed by slow locking.

*A Subtler Flytrap*—Despite the overall kinetic and structural similarities between S1S2 and the PBP, solution scattering data show that S1S2-agonist binding does not induce a large lobe closure equivalent to that seen for the PBP (33). Thus, instead of focusing on gross shifts between the lobes, as suggested by the Venus flytrap analogy, it is likely that smaller structural shifts within S1S2 will prove sufficient for inducing activation and desensitization. However, previous mutagenesis data (*e.g.* Refs. 29, 38, 49, and 50) and our kinetic results have identified residues on both sides of the cleft that interact with agonist. Interestingly, in S1S2, agonists are apparently able to interact with both lobes even in the absence of a dramatic relative motion due to an important structural difference between the orientations of ligands bound to S1S2 and the PBP. Here, for the first time, we can also assign an order of interaction to certain side chains involved in the binding process.

The homologs of $Glu^{403}$ and $Tyr^{451}$ sandwich the ligand side chain in a variety of amino acid-binding PBP, including the glutamine-binding protein (QBP) that is most closely related to the S1S2 core (Fig. 4*C*) (21, 25, 57, 58). PBP-bound amino acids thus lie roughly parallel to the hinge of the cleft (*i.e.* roughly horizontal in Fig. 4*C*). In contrast, in the kainate·S1S2 complex, the kainate "side chain" is directed almost at right angles to this orientation, brushing past $Tyr^{451}$ as its terminal carboxyl methyl group interacts with side chains from lobe II (Fig. 4*A*). As shown in Fig. 4*B*, glutamate may adopt a similar orientation, lying across rather than along the cleft, enabling it to interact with both sides in the absence of a dramatic closure. The $\alpha$-amino group bound deep within the cleft is also positioned so that only small rearrangements are apparently required to enable the recruitment of $Glu^{706}$ into a hydrogen-bonding network that spans both lobes and the agonist. This explains how agonists could be capable of linking the lobes of S1S2 together utilizing only subtle conformational changes within the domain. These small motions can then trigger subsequent conformational changes that open and close the channel pore. There is precedent for such subtlety both among the repressor protein-binding domains, whose conformational changes appear restricted by the need to maintain oligomeric interactions (31), and among PBP involved in transport (30, 59).

*Acknowledgments*—We thank U. Reygers for skillful technical assistance. We thank M. Geeves (Max Planck Institute for Molecular Physiology, Dortmund, Germany) for the pressure-jump experiments. We thank J. Reinstein (Max Planck Institute for Molecular Physiology, Dortmund) and J. Wray for suggestions on improving the manuscript.

REFERENCES

1. Nakanishi, S. (1992) *Science* **258,** 597–603
2. Sommer, B., and Seeburg, P. H. (1992) *Trends Neurosci.* **13,** 291–296
3. Keinänen, K., Wisden, W., Sommer, B., Werner, P., Herb, A., Verdoorn, T. A., Sakmann, B., and Seeburg, P. H. (1990) *Science* **249,** 556–560
4. Hollmann, M., and Heinemann, S. (1994) *Annu. Rev. Neurosci.* **17,** 31–108
5. Colquhoun, D., Jonas, P., and Sakmann, B. (1992) *J. Physiol. (Lond.)* **458,** 261–287
6. Seeburg, P. H. (1993) *Trends Neurosci.* **16,** 359–365
7. Kiskin, N. I., Krishtal, O. A., and Tsyndrenko, A. (1986) *Neurosci. Lett.* **63,** 225–230

[3] R. Abele and M. Geeves, unpublished data.

8. Mayer, M. L., and Vyklicky, L., Jr. (1989) *Proc. Natl. Acad. Sci. U. S. A.* **86,** 1411–1415
9. Tang, C. M., Dichter, M., and Morad, M. (1989) *Science* **243,** 1474–1477
10. Vyklicky, L. J., Patneau, D. K., and Mayer, M. L. (1991) *Neuron* **7,** 971–984
11. Trussell, L. O., Zhang, S., and Raman, I. M. (1993) *Neuron* **10,** 1185–1196
12. Yamada, K. A., and Tang, C. M. (1993) *J. Neurosci.* **13,** 3904–3915
13. Larson, J., Le, T. T., Hall, R. A., and Lynch, G. (1994) *Neuroreport* **5,** 389–392
14. Stern-Bach, Y., Bettler, B., Hartley, M., Sheppard, P. O., O'Hara, P. J., and Heinemann, S. F. (1994) *Neuron* **13,** 1345–1357
15. Miyazawa, A., Fujiyoshi, Y., Stowell, M., and Unwin, N. (1999) *J. Mol. Biol.* **288,** 765–786
16. Colquhoun, D., and Sakmann, B. (1998) *Neuron* **20,** 381–387
17. Kuusinen, A., Arvola, M., and Keinänen, K. (1995) *EMBO J.* **14,** 6327–6332
18. O'Hara, P. J., Sheppard, P. O., Thogersen, H., Venezia, D., Haldeman, B. A., McGrane, V., Houamed, K. M., Thomsen, C., Gilbert, T. L., and Mulvihill, E. R. (1993) *Neuron* **11,** 41–52
19. Wo, Z. G., and Oswald, R. E. (1995) *Trends Neurosci.* **18,** 161–168
20. Nakanishi, N., Schneider, N. A., and Axel, R. (1990) *Neuron* **5,** 569–581
21. Armstrong, N., Sun, Y., Chen, G.-Q., and Gouaux, J. E. (1998) *Nature* **395,** 913–916
22. Shilton, B. H., Flocco, M. M., Nilsson, M., and Mowbray, S. L. (1996) *J. Mol. Biol.* **264,** 350–363
23. Newcomer, M. E., Lewis, B. A., and Quiocho, F. A. (1981) *J. Biol. Chem.* **256,** 13218–13222
24. Olah, G. A., Trakhanov, S., Trewhella, J., and Quiocho, F. A. (1993) *J. Biol. Chem.* **268,** 16241–16247
25. Oh, B. H., Pandit, J., Kang, C. H., Nikaido, K., Gokcen, S., Ames, G. F. L., and Kim, S. H. (1993) *J. Biol. Chem.* **268,** 11348–11355
26. Sack, J. S., Saper, M. A., and Quiocho, F. A. (1989) *J. Mol. Biol.* **206,** 171–191
27. Mao, B., Pear, M. R., McCammon, J. A., and Quiocho, F. A. (1982) *J. Biol. Chem.* **257,** 1131–1133
28. Laube, B., Hirai, H., Sturgess, M., Betz, H., and Kuhse, J. (1997) *Neuron* **18,** 493–503
29. Mano, I., Lamed, Y., and Teichberg, V. I. (1996) *J. Biol. Chem.* **271,** 15299–15302
30. Sharff, A. J., Rodseth, L. E., and Quiocho, F. A. (1993) *Biochemistry* **32,** 10553–10559
31. Mowbray, S. L., and Björkman, A. J. (1999) *J. Mol. Biol.* **294,** 487–499
32. Patneau, D. K., Vyklicky, L., Jr., and Mayer, M. L. (1993) *J. Neurosci.* **13,** 3496–3509
33. Abele, R., Svergun, D., Keinänen, K., Koch, M. J. H., and Madden, D. R. (1999) *Biochemistry* **38,** 10949–10957
34. Abele, R. (1998) *Biochemische und Biophysikcalische Charakterisiervng Extrazellulärer Fragmente der Ionotropen Glutamatrezeptoruntereinheit GluRD*. Ph.D. thesis, Ruprecht-Karls-Universität, Heidelberg, Germany
35. Ledvina, P. S., Tsai, A.-L., Wang, Z., Koehl, E., and Quiocho, F. A. (1998) *Protein Sci.* **7,** 2550–2559
36. Vermersch, P. S., Tesmer, J. J. G., Lemon, D. D., and Quiocho, F. A. (1990) *J. Biol. Chem.* **265,** 16592–16603
37. Abele, R., Lampinen, M., Keinänen, K., and Madden, D. R. (1998) *J. Biol. Chem.* **273,** 25132–25138
38. Lampinen, M., Pentikäinen, O., Johnson, M. S., and Keinänen, K. (1998) *EMBO J.* **17,** 4704–4711, and references therein
39. Hiromi, K. (1979) *Kinetics of Fast Enzyme Reactions*, pp. 187–286, Halsted Press, New York
40. Wallace, A. C., Laskowski, R. A., and Thornton, J. M. (1995) *Protein Eng.* **8,** 127–134
41. Jones, T. A., Zou, J.-Y., and Cowan, S. W. (1991) *Acta Crystallogr. Sect. A* **47,** 110–119
42. Ponder, J. W., and Richards, F. M. (1987) *J. Mol. Biol.* **193,** 775–791
43. Weiner, J. H., and Heppel, L. A. (1971) *J. Biol. Chem.* **246,** 6933–6941
44. Miller, D. M., III, Olson, J. S., Pflugrath, J. W., and Quiocho, F. A. (1983) *J. Biol. Chem.* **258,** 13665–13672
45. Clements, J. D., Feltz, A., Sahara, Y., and Westbrook, G. L. (1998) *J. Neurosci.* **18,** 119–127
46. Lester, R. A. J., Tong, G., and Jahr, C. E. (1993) *J. Neurosci.* **13,** 1088–1096
47. Arai, A., Silberg, J., Kessler, M., and Lynch, G. (1995) *Neuroscience* **66,** 815–827
48. Jayaraman, V. (1998) *Biochemistry* **37,** 16735–16740
49. Uchino, S., Sakimura, K., Nagahari, K., and Mishina, M. (1992) *FEBS Lett.* **308,** 252–257
50. Paas, Y., Eisenstein, M., Medevielle, F., Teichberg, V. I., and Devillers-Thiery, A. (1996) *Neuron* **17,** 979–990
51. Hirai, H., Kirsch, J., Laube, B., Betz, H., and Kuhse, J. (1996) *Proc. Natl. Acad. Sci. U. S. A.* **93,** 6031–6036
52. Wafford, K. A., Kathoria, M., Bain, C. J., Marshall, G., Le Bourdelles, B., Kemp, J. A., and Whiting, P. J. (1995) *Mol. Pharmacol.* **47,** 374–380
53. Kawamoto, S., Uchino, S., Xin, K.-Q., Hattori, S., Hamajima, K., Fukushima, J., Mishina, M., and Okuda, K. (1997) *Mol. Brain Res.* **47,** 339–344
54. Williams, K., Chao, J., Kashiwagi, K., Masuko, T., and Igarashi, K. (1996) *Mol. Pharmacol.* **50,** 701–708
55. Walmsley, A. R., Shaw, J. G., and Kelly, D. J. (1992) *J. Biol. Chem.* **267,** 8064–8072
56. Saper, M. A., and Quiocho, F. A. (1983) *J. Biol. Chem.* **258,** 11057–11062
57. Yao, N. H., Trakhanov, S., and Quicho, F. A. (1994) *Biochemistry* **33,** 4769–4779
58. Sun, Y.-J., Rose, J., Wang, B.-C., and Hsiao, C.-D. (1998) *J. Mol. Biol.* **278,** 219–229
59. Lawrence, M. C., Pilling, P. A., Epa, V. C., Berry, A. M., Ogunniyi, A. D., and Paton, J. C. (1998) *Structure* **6,** 1553–1561